

Prevention of Lethal Murine Hypophosphatasia by Neonatal *Ex Vivo* Gene Therapy Using Lentivirally Transduced Bone Marrow Cells

Osamu Iijima,¹ Koichi Miyake,^{1,*} Atsushi Watanabe,^{1,2} Noriko Miyake,¹ Tsutomu Igarashi,^{1,3} Chizu Kanokoda,¹ Aki Nakamura-Takahashi,¹ Hideaki Kinoshita,⁴ Taku Noguchi,⁵ Shinichi Abe,⁵ Sonoko Narisawa,⁶ José Luis Millán,⁶ Takashi Okada,¹ and Takashi Shimada¹

¹Division of Gene Therapy, Department of Biochemistry and Molecular Biology, Research Center for Advanced Medical Technology, Nippon Medical School, Tokyo, Japan; ²Division of Clinical Genetics and ³Department of Ophthalmology, Nippon Medical School Hospital, Tokyo, Japan; Departments of ⁴Dental Materials Science and ⁵Anatomy, Tokyo Dental College, Tokyo, Japan; ⁶Sanford Children's Health Research Center, Sanford-Burnham Medical Research Institute, La Jolla, California.

Hypophosphatasia (HPP) is an inherited skeletal and dental disease caused by loss-of-function mutations in the gene that encodes tissue-nonspecific alkaline phosphatase (TNALP). The major symptoms of severe forms of the disease are bone defects, respiratory insufficiency, and epileptic seizures. In 2015, enzyme replacement therapy (ERT) using recombinant bone-targeted TNALP with deca-aspartate (D₁₀) motif was approved to treat pediatric HPP patients in Japan, Canada, and Europe. However, the ERT requires repeated subcutaneous administration of the enzyme because of the short half-life in serum. In the present study, we evaluated the feasibility of neonatal *ex vivo* gene therapy in TNALP knockout (*Akp2*^{-/-}) HPP mice using lentivirally transduced bone marrow cells (BMC) expressing bone-targeted TNALP in which a D₁₀ sequence was linked to the C-terminus of soluble TNALP (TNALP-D₁₀). The *Akp2*^{-/-} mice usually die within 20 days because of growth failure, epileptic seizures, and hypomineralization. However, an intravenous transplantation of BMC expressing TNALP-D₁₀ (ALP-BMC) into neonatal *Akp2*^{-/-} mice prolonged survival of the mice with improved bone mineralization compared with untransduced BMC-transplanted *Akp2*^{-/-} mice. The treated *Akp2*^{-/-} mice were normal in appearance and experienced no seizures during the experimental period. The lentivirally transduced BMC were efficiently engrafted in the recipient mice and supplied TNALP-D₁₀ continuously at a therapeutic level for at least 3 months. Moreover, TNALP-D₁₀ overexpression did not affect multilineage reconstitution in the recipient mice. The plasma ALP activity was sustained at high levels in the treated mice, and tissue ALP activity was selectively detected on bone surfaces, not in the kidneys or other organs. No ectopic calcification was observed in the ALP-BMC-treated mice. These results indicate that lentivirally transduced BMC can serve as a reservoir for stem cell-based ERT to rescue the *Akp2*^{-/-} phenotype. Neonatal *ex vivo* gene therapy thus appears to be a possible treatment option for treating severe HPP.

INTRODUCTION

HYPOPHOSPHATASIA (HPP) IS AN INHERITED skeletal and dental disease caused by mutations in the tissue-nonspecific alkaline phosphatase (TNALP) gene (*ALPL*).^{1,2} TNALP is a cell surface enzyme abundantly localized on the outer cell membrane of osteoblasts and chondrocytes and on the surface of their released matrix vesicles.³ The absence of functional TNALP in HPP results in extracellular accumulation of its natural substrates, which

include inorganic pyrophosphate (PP_i), pyridoxal 5'-phosphate and phosphoethanolamine.⁴ In addition, TNALP deficiency also leads to a hypomineralization of bones and teeth because of strong inhibition of hydroxyapatite crystal growth caused by accumulation of extracellular PP_i.²⁻⁴

All forms of HPP are usually diagnosed by first assaying serum alkaline phosphatase (ALP) activity, at least at the beginning of the diagnostic work-up. TNALP is thought to be released into the

*Correspondence: Dr. Koichi Miyake, Department of Biochemistry and Molecular Biology, Nippon Medical School, 1-1-5 Sendagi, Bunkyo-ku, Tokyo 113-8602, Japan. E-mail: kmiyake@nms.ac.jp

blood stream through phosphatidylinositol-specific phospholipase-catalyzed cleavage of its TNALP-glycosylphosphatidyl-inositol (GPI) anchoring motif.^{2,5} The clinical manifestations of HPP vary widely, and the disease was recently classified into six forms based on its severity and age at diagnosis.¹ The perinatal and infantile forms of HPP are severe and often fatal. The major symptoms of severe HPP are bone defects, respiratory insufficiency, and epileptic seizures.^{6,7} The impaired bone mineralization caused by TNALP deficiency leads to bone defects that make these patients prone to bone fracture, and the most severely affected patients endure intubation and mechanical ventilation to relieve respiratory insufficiency because of rib cage dysplasia. In addition, pyridoxine-responsive seizures often occur in infantile HPP.⁸

Clinical studies of transplantation therapy for severe HPP have been conducted using allogeneic bone marrow cells (BMC), mesenchymal stem cells (MSC), and cultured osteoblasts.^{9–12} The rationale of these protocols is that donor cells may distribute and engraft in the skeletal microenvironment to differentiate into osteoprogenitor cells synthesizing physiologically active TNALP. With these approaches, therapeutic benefits such as improved bone mineralization were observed, but the biochemical markers, including serum ALP activity, were not corrected.^{9–12} Further studies aimed at further improving the therapeutic effect are thus needed.

Millán and colleagues reported that enzyme replacement therapy (ERT) using recombinant bone-targeted TNALP with the Fc region of human IgG and a bone targeting deca-aspartate (D₁₀) motif at the enzyme's C-terminus prevented disease in the TNALP knockout (*Akp2*^{-/-}) mouse model of infantile HPP.¹³ These findings underpinned the phase I/II clinical trials of ERT using the recombinant bone-targeted TNALP (asfotase alfa; Alexion Pharmaceuticals) to treat perinatal and infantile HPP patients.¹⁴ Subsequently, asfotase alfa was approved for treatment of pediatric HPP in Japan, Canada, and Europe. Other potential ERTs using GPI-anchorless TNALP¹⁵ or intestinal-like chimeric alkaline phosphatase¹⁶ to prevent HPP in *Akp2*^{-/-} mice have been reported. However, because these biologics have a short half-life in serum, ERT for HPP requires repeated subcutaneous injections of the enzyme.¹⁴

Taking a different approach to treating HPP, we demonstrated that a single intravenous or intraperitoneal injection of a lentiviral or adeno-associated viral (AAV) vector encoding bone-targeted TNALP in which D₁₀ was linked adjacent to the C-terminus of

soluble TNALP (*TNALP-D*₁₀) resulted in sustained expression of TNALP-D₁₀ and prevention of the disease phenotype in *Akp2*^{-/-} mice.^{17–19} Viral vector-mediated ERT should be more practical and economical than classic ERT, which requires repeated injection of purified recombinant enzyme. There are several concerns with this *in vivo* gene therapy, however, including the risk of inadvertent germline gene transfer^{20,21} and induction of immune responses to the viral vector peptide or transgene product^{22,23} after systemic or tissue-specific administration of the high-dose viral vector needed to achieve therapeutic benefits.

An alternative gene therapy approach is BMC-mediated *ex vivo* gene therapy. Up to now, no *ex vivo* gene therapy protocols have been approved; however, several clinical trials of BMC-mediated *ex vivo* gene therapy have been conducted to treat not only hematological diseases^{24,25} but also inherited lysosomal storage disorders.^{26–28} Lysosomal enzymes are secreted and recaptured by the surrounding cells. Accordingly, the goal of this approach is to provide a reservoir of lysosomal enzyme *in vivo*. Lentivirally transduced BMC showed robust, long-term expression of the transgene, and provided the therapeutic enzyme in appreciable levels for correction of the symptoms.^{26–28} In addition, with *ex vivo* gene therapy the risks of incidental germline gene transfer and induction of an immunoreaction against the viral vector are eliminated.²⁹ Although the oncogenicity of conventional integrating viral vectors used for *ex vivo* gene therapy is a concern, the genotoxicity is now minimized through several safety modifications.^{29,30} In that context, we reasoned that HPP could also be treated by BMC-mediated *ex vivo* gene therapy. Moreover, these strategies would be applicable not only to inherited bone disorders, including HPP, but also to other diseases that could be treated using ERT.

In the present study, therefore, we examined the feasibility of neonatal *ex vivo* gene therapy using genetically modified BMC as an approach to treatment of HPP. On day 2 after birth, we performed a single systemic transplantation of lentivirally transduced BMC expressing TNALP-D₁₀ to treat the lethal phenotype of *Akp2*^{-/-} mice.

MATERIALS AND METHODS

Mice

Akp2^{-/-} mice, which phenotypically mimic infantile HPP, were created as previously described.³¹ These mice usually appear normal at birth but die within 20 days while exhibiting serious growth failure and skeletal hypomineralization.³² The

major cause of death is apnea, most likely resulting from their severe epileptic seizures. Breeding heterozygous (*Akp2*^{+/-}) pairs, their pups, and weanlings were fed a rodent diet supplemented with 325 ppm pyridoxine (Oriental Yeast Co., Ltd., Tokyo, Japan). The pyridoxine supplementation delayed the onset of epileptic attacks and extended their survival.³² *Akp2* genotyping was done using PCR with primers 5'-AGTCCGTGGGCATTGTGACTA-3' and 5'-TGCTGCTCCACTCACGTCGAT-3'.¹⁷ B6.CD45.1 (*Akp2*^{+/+}) mice were purchased from Sankyo Labo Service Co., Inc. (Tokyo, Japan) and used as donors for bone marrow transplantation. The haplotypes of the Ly5 antigens of *Akp2*^{-/-} and B6.CD45.1 mice are Ly5.2 and Ly5.1, respectively. All animal experiments were carried out with approval from the Nippon Medical School Animal Ethics Committee.

Cell culture

The 293T and HeLa cell lines were cultured in Dulbecco's modified Eagle's medium supplemented with 10% fetal bovine serum (FBS), 50 U/ml penicillin, and 50 µg/ml streptomycin under an atmosphere enriched with 5% CO₂.

BMC preparation was performed as described previously.³³ In brief, BMC were harvested from the femurs and tibiae of 8–12-week-old B6.CD45.1 mice. Lineage-negative (Lin⁻) BMC were enriched using a Mouse Hematopoietic Progenitor (Stem) Cell Enrichment Set (BD Biosciences, Franklin Lakes, NJ) following manufacturer's instructions. The Lin⁻ BMC were then prepared at the density of 1 × 10⁶ cells/ml in X-Vivo medium (X-Vivo15; Takara Bio Inc., Shiga, Japan) supplemented with 1% bovine serum albumin (Sigma-Aldrich, St. Louis, MO), 0.1 mM β-mercaptoethanol (Invitrogen, Life Technology Japan, Tokyo, Japan), 2 mM L-glutamine (Invitrogen), 100 units/ml penicillin, 100 µg/ml streptomycin (Invitrogen), 50 ng/ml murine stem cell factor (R&D Systems, Minneapolis, MN), 10 ng/ml murine interleukin-3 (R&D Systems), and 50 ng/ml human interleukin-6 (R&D Systems).

Lentiviral vector preparation and transduction

The lentiviral vector plasmids carrying cDNA for *TNALP-D*₁₀¹⁹ or enhanced green fluorescent protein (*EGFP*)³⁴ have been described previously. The lentiviral genome contains a reverse-oriented, 0.25 kb insulator element from the 5' hypersensitive site 4 (5'HS4) of the chicken β-globin gene (cHS4 insulator) within the U3 region of the self-inactivating long terminal repeat (SIN-LTR), which blocks unintended enhancer effects of the

internal promoter. Expression of *TNALP-D*₁₀ or *EGFP* was under the control of the U3 region of the murine stem cell virus LTR (MSCV-U3) acting as an internal promoter. The lentiviral vector was prepared by transient transfection of 293T cells as previously described.³⁴ The titer of the vector stock was determined in HeLa cells by measuring the copy number of the integrated vector genome using real-time PCR (7500 Fast; Applied Biosystems, Carlsbad, CA), and was expressed as transducing units per milliliter (TU/ml). Thereafter, 1 × 10⁶ Lin⁻ BMC were transferred to Retronectin (Takara Bio Inc.)-coated 24-well plates and transduced with the lentiviral vector carrying the *TNALP-D*₁₀ gene (ALP-BMC) or *EGFP* gene (GFP-BMC) by incubation for 20 hr at 37°C at a multiplicity of infection of 50.

Colony-forming unit assay

Colony-forming unit (CFU) assay was performed as described previously.³³ In brief, 2 × 10³ transduced or untransduced Lin⁻ BMC in 1 ml of MethoCult M3534 (Stem Cell Technologies, Vancouver, BC, Canada) were seeded into 6-well culture plates. CFU-macrophage (CFU-M) and CFU-granulocyte-macrophage (CFU-GM) colonies were then scored on day 7. All assays were performed in triplicate.

BMC transplantation

Four hours before transplantation on postnatal day 2, neonatal *Akp2*^{-/-} mice were conditioned with a single 4 Gy dose of total body irradiation (TBI) using an X-ray machine (MBR-1505R2, Hitachi Medical Co., Tokyo, Japan). The mice were then transplanted with 1 × 10⁶ transduced or untransduced Lin⁻ BMC intravenously via the jugular vein or superficial temporal vein using a 29-gauge insulin syringe.

Engraftment and lineage analysis of peripheral blood

Using a heparinized hematocrit capillary tube (Terumo Corp., Tokyo, Japan), peripheral blood (PB) was collected from the retro-orbital plexus of recipient mice approximately every 30 days following transplantation. The erythrocytes were then lysed with NH₄Cl, and the remaining cells were washed once with PBS. To then measure the donor cell engraftment rate, PB mononuclear cells (PBMC) were resuspended in PBS containing 5% FBS and incubated first with biotin-conjugated antibodies directed against murine CD45.1 (Ly5.1) for 30 min at 4°C and then with Streptavidin-FITC. In addition, PE-conjugated antibodies directed against murine Mac-1 (monocytes), Gr-1 (granulocytes), B220 (B-cells), and CD3e (T-cells) were

used together to analyze multilineage potency.³³ All monoclonal antibodies used were purchased from BD Biosciences. The cells were then subjected to FACS analysis using a FACScalibur flow cytometer (BD Biosciences).

Colorimetric ALP activity assay

ALP activity was determined as previously described.¹⁷ One unit (U) was defined as the amount of enzyme needed to catalyze production of 1 μ mol of p-nitrophenol per minute, and ALP activity in plasma and cell culture supernatants was calculated as U/ml. PB was collected 1 week after transplantation via the tail vein. In addition, the brain, heart, liver, spleen, kidney, and bone (a mixture of bone and bone marrow) were harvested after perfusing mice with 20 ml of PBS containing 10 U/ml of heparin under deep anesthesia. The organs were then homogenized using the Percellys-24 bead-beating homogenizer according to the company's protocol (Bertin Technologies, Paris, France), and the supernatants of homogenates were used to measure tissue ALP activity. After measuring the protein concentration using a DC protein assay kit (Bio-Rad, Hercules, CA), ALP activity was expressed per milligram (mg) protein.

Biodistribution of lentiviral vector

Genomic DNA was extracted from tissue homogenates using a Gentra Puregene Kit (Qiagen, Venlo, The Netherlands) and then subjected to real-time PCR to estimate the vector distribution. The primer/probe set LentiP.F (5'-CAG GAC TCG GCT TGC TGA AG-3'), LentiP.R (5'-TCC CCC GCT TAA TAC TGA CG-3') and TaqMan probe LentiP.P (5'-FAM-CGC ACG GCA AGA GGC GAG G-TAMRA-3') was used to detect the lentiviral vector provirus, as described previously.³⁵ A TaqMan Copy Number Reference Assay, Mouse, Tfrc (transferrin receptor) VIC-TAMRA probe (Applied Biosystems) was used to quantify the genomic DNA. To estimate the vector distribution, genomic DNA from wild-type (*Akp2*^{+/+}) mice spiked with plasmid DNA was used as a standard, and the average copy number per diploid was determined. Assays were performed in triplicate on an ABI 7500Fast Real-Time PCR System (Applied Biosystems) using the following protocol: 1 cycle of 10 min at 95°C followed by 40 cycles of 15 sec at 95°C and 1 min at 60°C.

Histochemical ALP activity staining

Knee joints were removed and embedded in SCEM compound (Leica Microsystems, Tokyo, Japan) without fixation or decalcification and stored at -80°C. For study, sections (7 μ m thick)

were cut using the Kawamoto film method³⁶ and fixed with 4% paraformaldehyde. ALP activity was assayed by incubating the tissue in 20 ml of 0.1 M Tris-HCl buffer (pH 8.5) containing 0.1 mg/ml naphthol AS-MX phosphate, which served as the substrate, and 0.3 mg/ml fast blue BB salt for 15 min at 37°C, as described previously.¹⁷ After washing away excess buffer with distilled H₂O, the tissue sections were mounted on silane-coated slides (Muto Pure Chemicals, Ltd., Tokyo, Japan) and examined under a light microscope (BX 60; Olympus Ltd., Tokyo, Japan).

X-ray analysis

Radiographic images were acquired using a μ FX-1000 X-ray unit (Fujifilm, Tokyo, Japan) and analyzed with an FLA-7000 image reader (Fujifilm). The X-ray energy level was 25 kV, and the exposure time was 30 sec.¹⁷

Microcomputed tomography

To analyze the femoral bone morphology, high-resolution microcomputed tomography (μ CT) was carried out using a HMX-225 Actis4 system (Tesco Co., Tokyo, Japan).³⁷ The samples were moistened with PBS and scanned at 15 \times magnification using a slice width of 50 μ m, matrix size of 512 \times 512, slice pitch of 50 μ m, and voxel size of 23 \times 23 \times 50 μ m, applying an energy level of 120 kV and intensity of 83 μ A. The digital images obtained were processed to reconstruct 3D structures using reconstruction software (VG Studio; Volume Graphics Co. Ltd., Heidelberg, Germany). The 3D structure of trabecular bone was evaluated in a 0.5-mm-thick section of the distal metaphysis region adjacent to the growth plate. The bone morphometric parameters were calculated using TRI/3D-BON software (Ratoc System Engineering Inc., Tokyo, Japan).

Statistical analysis

Data are presented as mean \pm standard deviation (SD). Differences between means were tested for statistical significance using Student's *t*-test. Values of *p* < 0.05 were considered significant. Survival rates were analyzed using the Kaplan-Meier method, and a log-rank test was used to assess the survival differences. Statistical analyses were performed with IBM SPSS Statistics Version 20 (IBM Corp., Tokyo, Japan).

RESULTS

Prolonging survival of *Akp2*^{-/-} mice through neonatal transplantation of BMC expressing TNALP-D₁₀

In this study, we compared the therapeutic effects of transplantation of lentivirally transduced

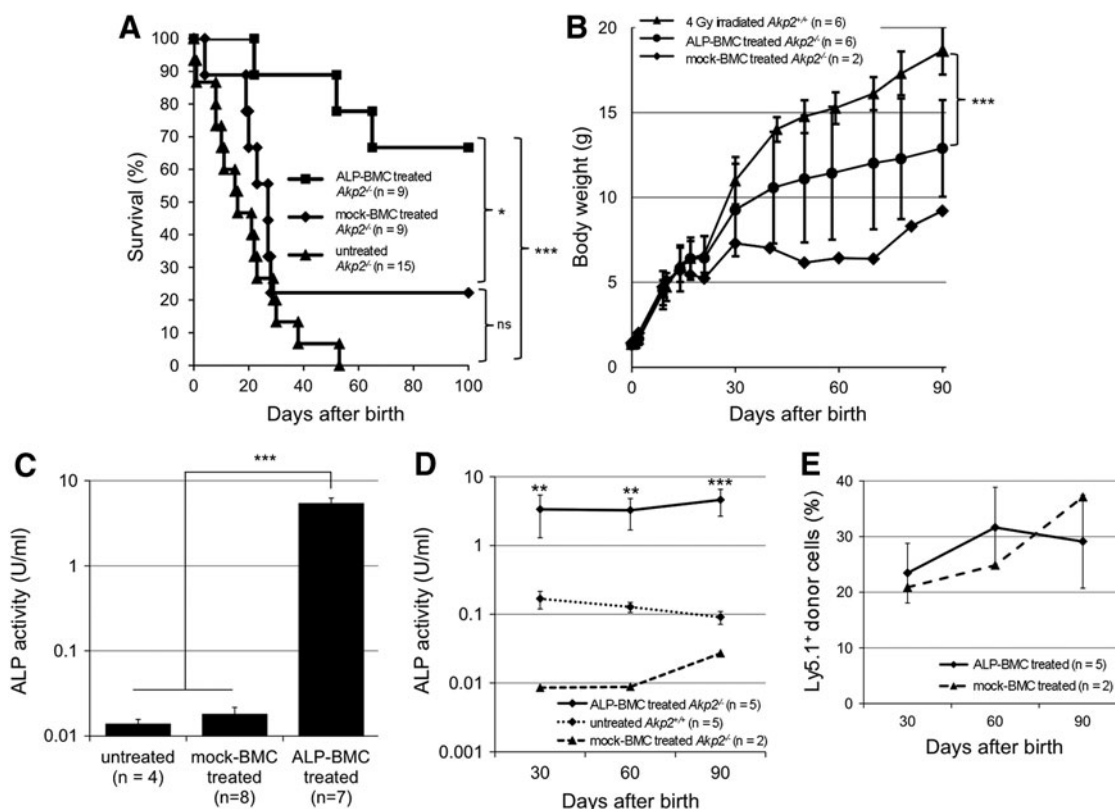


Figure 1. Therapeutic effects of *ex vivo* gene therapy in neonatal *Akp2*^{-/-} mice. **(A)** Survival curves for ALP-BMC-treated, mock-BMC-treated, and untreated *Akp2*^{-/-} mice. **p* < 0.05, ALP-BMC-treated vs. mock BMC-treated *Akp2*^{-/-} mice; ****p* < 0.001, ALP-BMC-treated vs. untreated *Akp2*^{-/-} mice; ns, not significant (*p* = 0.14, mock BMC-treated vs. untreated *Akp2*^{-/-} mice). **(B)** Comparison of average body weights among *Akp2*^{+/+} mice irradiated at a dose of 4 Gy, ALP-BMC-treated *Akp2*^{-/-} mice (4 Gy irradiation), and mock-BMC-treated *Akp2*^{-/-} mice (4 Gy irradiation). ****p* < 0.001, ALP-BMC-treated vs. 4 Gy-irradiated *Akp2*^{+/+} mice on day 90. **(C)** Comparison of plasma ALP activity 1 week after treatment among untreated (*n* = 4), mock-BMC-treated (*n* = 8), and ALP-BMC-treated (*n* = 7) *Akp2*^{-/-} mice. ****p* < 0.001 vs. ALP-BMC-treated *Akp2*^{-/-} mice. **(D)** Time course of the changes in plasma ALP activity in ALP-BMC-treated *Akp2*^{-/-} mice, untreated *Akp2*^{+/+} mice, and mock-BMC-treated *Akp2*^{-/-} mice. ***p* < 0.01, ****p* < 0.001, ALP-BMC-treated vs. untreated *Akp2*^{+/+} mice. **(E)** Long-term engraftment of Ly5.1⁺ donor cells in ALP-BMC-treated and mock-BMC-treated *Akp2*^{-/-} mice. ALP, alkaline phosphatase; BMC, bone marrow cells.

BMC expressing TNALP-D₁₀ (ALP-BMC) and untransduced BMC (mock-BMC), which were harvested from B6.CD45.1 (*Akp2*^{+/+}, Ly5.1) mice, for the treatment of neonatal *Akp2*^{-/-} mice. According to the titration studies, we determined 4 Gy of TBI as the sublethal dose for the neonatal transplantation. Neonatal mice irradiated with 4 Gy showed a moderate reduction in body weight compared with unirradiated neonatal mice, but no symptoms of acute radiation syndrome such as inhibition of hair growth, cataracts, or marked growth retardation (data not shown).

Following injection of mock-BMC into irradiated neonatal *Akp2*^{-/-} mice on day 2 after birth (mock-BMC-treated *Akp2*^{-/-} mice), seven of nine mice died within 1 month (Fig. 1A). The survival was narrowly prolonged in the remaining two mock-BMC-treated *Akp2*^{-/-} mice; however, this was not a significant effect, as compared with untreated *Akp2*^{-/-} mice (*p* = 0.14). By contrast, survival was significantly prolonged in neonatal *Akp2*^{-/-} mice

receiving ALP-BMC (ALP-BMC-treated *Akp2*^{-/-} mice), as compared with untreated *Akp2*^{-/-} mice (*p* < 0.001) and mock-BMC-treated *Akp2*^{-/-} mice (*p* < 0.05). The ALP-BMC-treated *Akp2*^{-/-} mice were normal in appearance and experienced no seizures during the experimental period. In addition, the growth curve for ALP-BMC-treated *Akp2*^{-/-} mice was significantly improved over that obtained with mock-BMC-treated *Akp2*^{-/-} mice (Fig. 1B). However, the body weight increase in ALP-BMC-treated *Akp2*^{-/-} mice did not reach the level seen with age-matched 4 Gy-irradiated *Akp2*^{+/+} mice (Fig. 1B).

Long-term enzyme supplementation from BMC expressing TNALP-D₁₀

To evaluate TNALP-D₁₀ expression in the ALP-BMC-treated *Akp2*^{-/-} mice, plasma ALP activity was measured 1 week and every 30 days after BMC transplantation. The plasma ALP activity rapidly increased in ALP-BMC-treated *Akp2*^{-/-} mice and

was approximately 400 times higher than in untreated *Akp2*^{-/-} mice within 1 week after transplantation (5.391 ± 2.285 vs. 0.014 ± 0.004 U/ml) (Fig. 1C). The plasma ALP activity of mock-BMC-treated *Akp2*^{-/-} mice (0.018 ± 0.011 U/ml) was essentially the same as in untreated *Akp2*^{-/-} mice. In addition, the plasma ALP activity in ALP-BMC-treated *Akp2*^{-/-} mice was sustained at significantly higher level than was seen in untreated *Akp2*^{+/+} mice throughout the experimental period (Fig. 1D). This is noteworthy, as the plasma ALP level was sufficient to obtain therapeutic benefits without adverse effects, as we reported previously.¹⁷⁻¹⁹ In both ALP-BMC-treated *Akp2*^{-/-} mice and the two surviving mock-BMC-treated *Akp2*^{-/-} mice, the engraftment of donor cells was maintained at approximately 30% throughout the experimental period (Fig. 1E), though only the ALP-BMC-treated *Akp2*^{-/-} mice experienced a therapeutic effect. These results indicate that transplantation of native BMC is not adequate to treat *Akp2*^{-/-} mice; genetic modification of the donor BMC is necessary for continuous supplementation of TNALP-D₁₀ at a level sufficient to obtain therapeutic effects.

Overexpression of TNALP-D₁₀ does not influence multilineage reconstitution in ALP-BMC-treated *Akp2*^{-/-} mice

The effect of TNALP-D₁₀ overexpression on the multilineage differentiation potential of lentivirally transduced BMC was assessed using CFU assays (Table 1). The numbers of CFU-M and CFU-GM did not differ among untreated BMC, ALP-BMC, and GFP-BMC. Transduction efficiency, based on the fraction of GFP-positive colonies among the total colonies formed by GFP-BMC, was $73.9 \pm 20.9\%$. The *in vivo* multilineage reconstitution of hematopoiesis (myeloid, B, and T-cells) in the ALP-BMC-treated *Akp2*^{-/-} mice was also assessed by FACS analysis on day 90 after transplantation (Table 2). Upon reconstitution, the lineage profile in PB from ALP-BMC-treated *Akp2*^{-/-} mice was similar to that in mock-BMC-treated *Akp2*^{+/+} mice. There was no disturbance in the numbers of circulating monocytes, neutrophils, or B and T lymphocytes, although the exogenous TNALP-D₁₀ was manufactured in the transduced bone marrow precursor cells. Moreover, the ratios of donor BMC in each lineage were similar between ALP-BMC-treated *Akp2*^{-/-} mice and mock-BMC-treated *Akp2*^{+/+} mice. These results indicate that long-term overexpression of TNALP-D₁₀ does not affect donor cell engraftment or multilineage reconstitution in the recipient mice.

Table 1. Colony-forming unit assay of bone marrow cells transduced by lentiviral vectors

Transduction	CFU-M	CFU-GM	Total
UT-BMC	11.7 ± 2.1	9.7 ± 3.2	21.3 ± 4.7
ALP-BMC	12.0 ± 1.7	9.3 ± 2.5	21.3 ± 3.2
GFP-BMC	12.7 ± 1.5	10.7 ± 5.9	23.3 ± 4.6

ALP, alkaline phosphatase; BMC, bone marrow cells; CFU, colony-forming unit; GFP, green fluorescent protein; GM, granulocyte macrophage; M, macrophage; UT, untransduced.

CFU colonies in methylcellulose culture were evaluated at day 7 ($n=3$). Data are presented as mean ± SD. No significant differences were observed.

Accumulation of TNALP-D₁₀ on the bone surface in ALP-BMC-treated *Akp2*^{-/-} mice

To examine ALP expression in the organs, selected tissues were harvested from untreated *Akp2*^{+/+} mice and untreated and ALP-BMC-treated *Akp2*^{-/-} mice on day 30 after transplantation. Colorimetric assays of ALP activity in the tissue homogenates revealed that bone ALP activity was significantly increased in ALP-BMC-treated *Akp2*^{-/-} mice, compared with untreated *Akp2*^{-/-} mice (Fig. 2A). The renal ALP activity, which was abundant in *Akp2*^{+/+} mice, was not restored in the ALP-BMC-treated *Akp2*^{-/-} mice. In the *Akp2*^{+/+} mice, native form of TNALP exists on the cell membrane surface, anchored by a GPI anchor motif. However, TNALP-D₁₀ secreted from the transduced cells has a high affinity for hydroxyapatite, and so the circulating TNALP-D₁₀ is thought to accumulate selectively on bone surfaces in ALP-BMC-treated *Akp2*^{-/-} mice, not in the kidneys. In addition, splenic ALP activity was only slightly elevated from the basal level, though the same high copy number of the lentiviral vector genome present in bone was also detected in the spleen (Fig. 2B). Furthermore, histological detection showed apparent ALP activity on the surface of trabecular and cortical bones in the distal femoral metaphysis of 30-day-old ALP-BMC-treated *Akp2*^{-/-} mice, whereas no ALP signal was detected in the corresponding area in

Table 2. Multilineage reconstitution in the peripheral blood of the transplanted mice

	% in total PBMC		
	Myeloid cell	B-cell	T-cell
ALP-BMC-treated <i>Akp2</i> ^{-/-} ($n=5$) (% donor in each lineages)	11.9 ± 4.2 (38.5 ± 7.5)	33.6 ± 20.7 (21.7 ± 9.9)	59.0 ± 17.3 (42.0 ± 9.6)
Mock-BMC-treated <i>Akp2</i> ^{+/+} ($n=3$) (% donor in each lineages)	9.6 ± 0.9 (49.3 ± 19.4)	32.9 ± 8.4 (29.1 ± 14.3)	55.7 ± 14.8 (57.1 ± 27.4)

PBMC, peripheral blood mononuclear cells.

Myeloid cells, B-cells, and T-cells were identified by PE-conjugated anti-mouse Mac-1 + Gr-1, B220, and CD3e antibodies, respectively, on day 90 after transplantation. Donor Ly5.1⁺ cells were identified by FITC-conjugated anti-mouse CD45.1 antibody. Data are presented as the mean ± SD. No significant differences were observed.

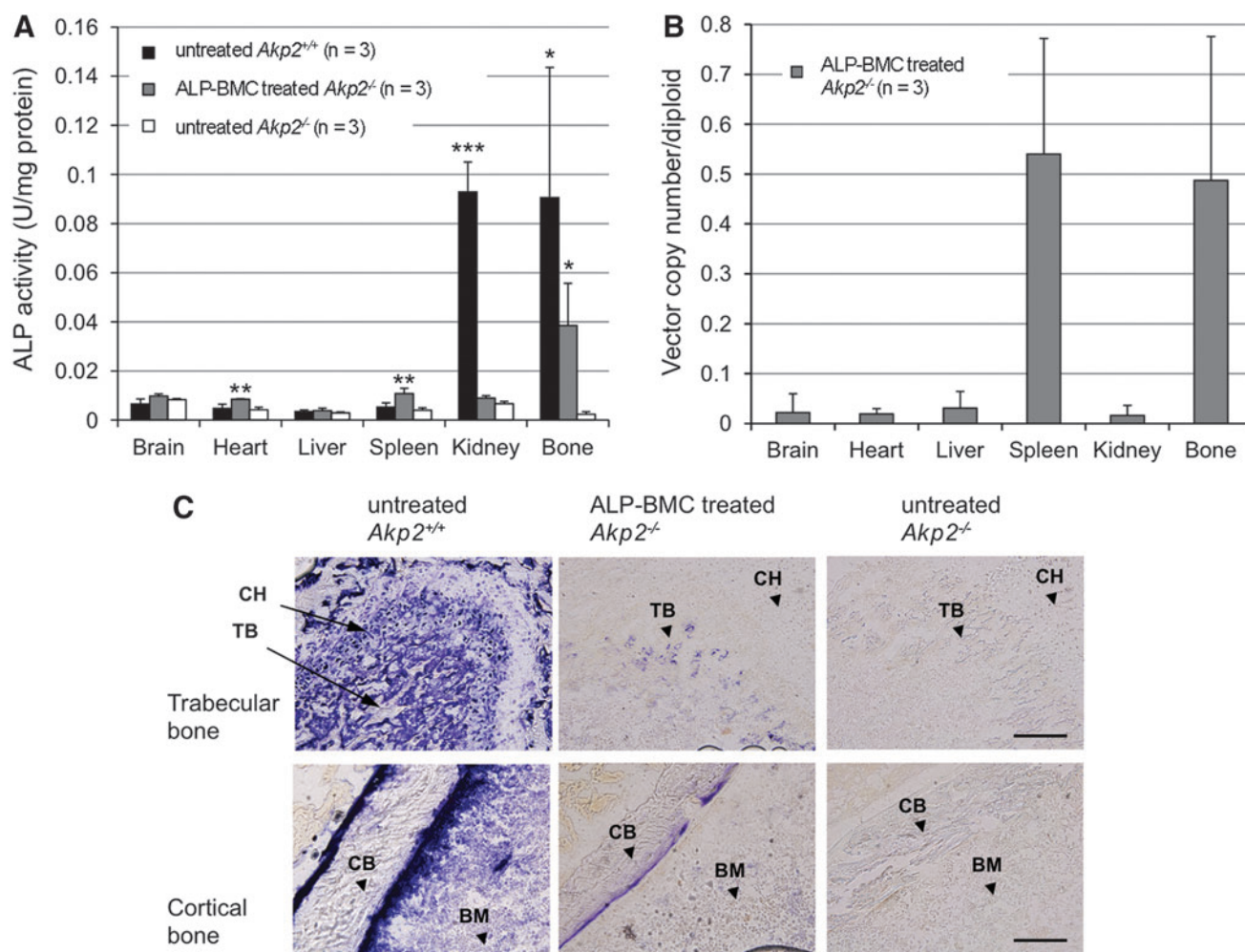


Figure 2. Tissue ALP activity and lentiviral vector distribution in ALP-BMC-treated *Akp2*^{-/-} mice. **(A)** Comparison of tissue ALP activity. ALP activities were measured in the supernatants from the indicated tissue homogenates using a colorimetric assay. Tissue samples were collected from untreated *Akp2*^{+/+} mice, ALP-BMC-treated *Akp2*^{-/-} mice, and untreated *Akp2*^{-/-} mice 30 days after transplantation ($n=3$, respectively). * $p < 0.05$, ** $p < 0.01$, *** $p < 0.001$ vs. untreated *Akp2*^{-/-} mice. **(B)** Distribution of the lentiviral vector genome in the tissues of ALP-BMC-treated *Akp2*^{-/-} mice ($n=3$). The presence of integrated vector genome was detected using real-time PCR with a lentiviral vector-specific TaqMan probe. Vector copy numbers were normalized to the *mTfrc* gene. **(C)** Histochemical staining of ALP activity in the femurs of 30-day-old untreated *Akp2*^{+/+} mice, ALP-BMC-treated *Akp2*^{-/-} mice, and untreated *Akp2*^{-/-} mice. ALP activity is reflected by blue staining on the surface of the trabecular and cortical bone. BM, bone marrow; CB, cortical bone; CH, chondrocyte; TB, trabecular bone. Scale bar: trabecular bone (upper panels), 200 μm ; cortical bone (lower panels), 100 μm .

untreated *Akp2*^{-/-} mice (Fig. 2C). No ectopic calcification was observed within internal organs or muscle upon macroscopic diagnosis or X-ray examination. These results indicate that bone-targeted TNALP-D₁₀ selectively accumulated on the bone surface, in agreement with its high affinity for hydroxyapatite,^{3,17} although the accumulated levels were much lower than those found in the *Akp2*^{+/+} mice (Fig. 2C).

Morphological analysis of bone structure in ALP-BMC-treated *Akp2*^{-/-} mice

The efficacy of *ex vivo* gene therapy for correction of bone hypomineralization was evaluated through X-ray and μCT examination of the hind limbs of 100-day-old untreated *Akp2*^{+/+} and ALP-BMC-

treated and mock-BMC-treated *Akp2*^{-/-} mice. Bone formation in ALP-BMC-treated *Akp2*^{-/-} mice was improved, as compared with mock-BMC-treated *Akp2*^{-/-} mice (Fig. 3A and B). The lack of bone formation in the proximal femoral diaphysis and secondary ossification centers in the hind paw was only seen in the mock-BMC-treated *Akp2*^{-/-} mice, although the lengths of the femur and tibia were nearly the same in ALP-BMC-treated and mock-BMC-treated *Akp2*^{-/-} mice (Fig. 3A). On the other hand, incomplete osteogenesis, such as a widened metaphysis, which is frequently observed in the HPP patients,^{38,39} persisted in both ALP-BMC-treated and mock-BMC-treated *Akp2*^{-/-} mice (Fig. 3B). Nonetheless, μCT analysis indicated that the

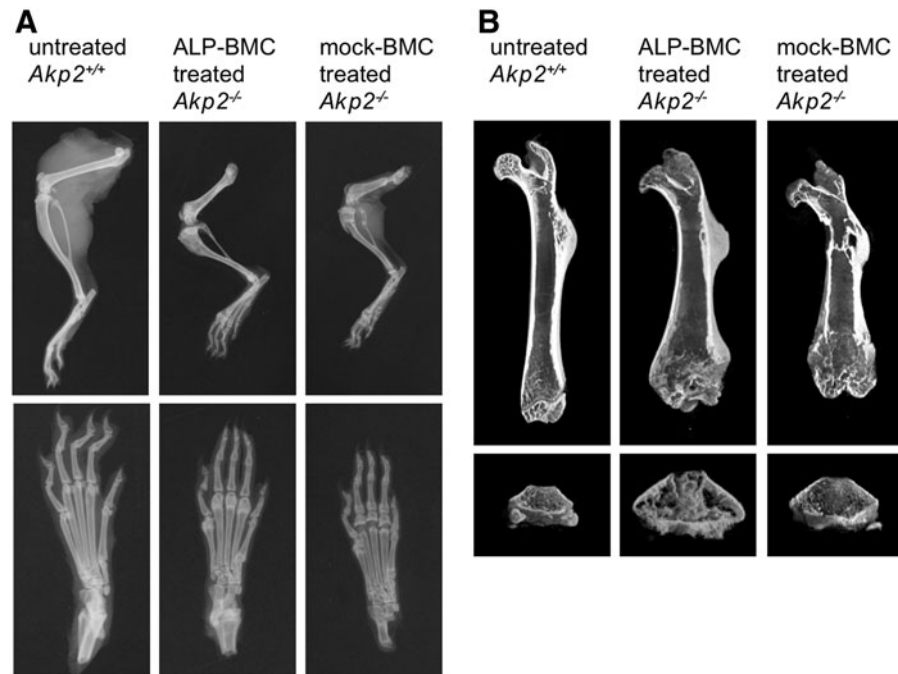


Figure 3. Hind limb bone morphology. Representative bone morphology in 100-day-old untreated $Akp2^{+/+}$ mice, ALP-BMC-treated $Akp2^{-/-}$ mice and mock-BMC-treated $Akp2^{-/-}$ mice. **(A)** X-ray radiographs of hind limbs (upper panels) and paws (lower panels). **(B)** μ CT 3D images of femurs (upper panels) and distal femoral metaphysis (lower panels). μ CT, micro-computed tomography.

bone morphology of ALP-BMC-treated $Akp2^{-/-}$ mice was markedly better than that of mock-BMC-treated $Akp2^{-/-}$ mice, and was similar to that in $Akp2^{+/+}$ mice (Fig. 4A and C–F), except for the bone mineral density (BMD) (Fig. 4B). These data indicate that bone structural development is improved in ALP-BMC-treated mice, although accumulation of minerals such as calcium remains insufficient.

DISCUSSION

In this study, we examined the feasibility of neonatal *ex vivo* gene therapy using lentivirally transduced BMC expressing TNALP-D₁₀ to rescue $Akp2^{-/-}$ mice, a model of infantile HPP. We found that gene therapy prevented the epileptic seizures otherwise were seen in $Akp2^{-/-}$ mice and significantly prolonged the survival of the mice, which also exhibited improved weight gain (Fig. 1A and B). In response to gene therapy, plasma ALP activity rapidly increased to therapeutically effective levels (Fig. 1C) and was sustained at the higher levels for more than 3 months (Fig. 1D). Collectively, these results indicate that a single neonatal transplantation of BMC expressing TNALP-D₁₀ provides significant therapeutic benefits and significantly prolongs the survival of $Akp2^{-/-}$ mice.

Seven of the nine mock-BMC-treated $Akp2^{-/-}$ mice died within 1 month (Fig. 1A), and the re-

maining two mock-BMC-treated $Akp2^{-/-}$ mice narrowly survived but with significant growth impairment (Fig. 1B). This may reflect a benefit provided by the transplanted mock-BMC¹² or by other phosphatases related to bone mineralization, such as PHOSPHO1 and nucleotide pyrophosphatase/phospho-diesterase-1, which could act to compensate for the absence of endogenous TNALP⁴⁰ and contribute to the relief of symptoms in the mock-BMC-treated $Akp2^{-/-}$ mice. In this experiment, we used B6.CD45.1 ($Akp2^{+/+}$, Ly5.1) mice as a donor for bone marrow transplantation because of difficulty of collecting BMC from $Akp2^{-/-}$ newborn mice and the utility of the Ly5.1 marker for detection of engrafted donor cells. Additional experiments using $Akp2^{-/-}$ BMC as donor cells may be needed to clarify the efficacy of bone marrow transplantation and *ex vivo* gene therapy for the treatment of HPP. On the other hand, the therapeutic efficacy of MSC and osteoblast transplantation has been reported.^{9–12} In addition, the differentiation of a patient's MSC into osteoblasts after transduction with a retroviral vector encoding native form of TNALP has also been reported.⁴¹ Based on those findings, we suggest that co-transplantation of genetically modified BMC and MSC could be an effective approach to treating HPP. Further studies will be needed to determine whether BMC expressing TNALP-D₁₀ for systemic

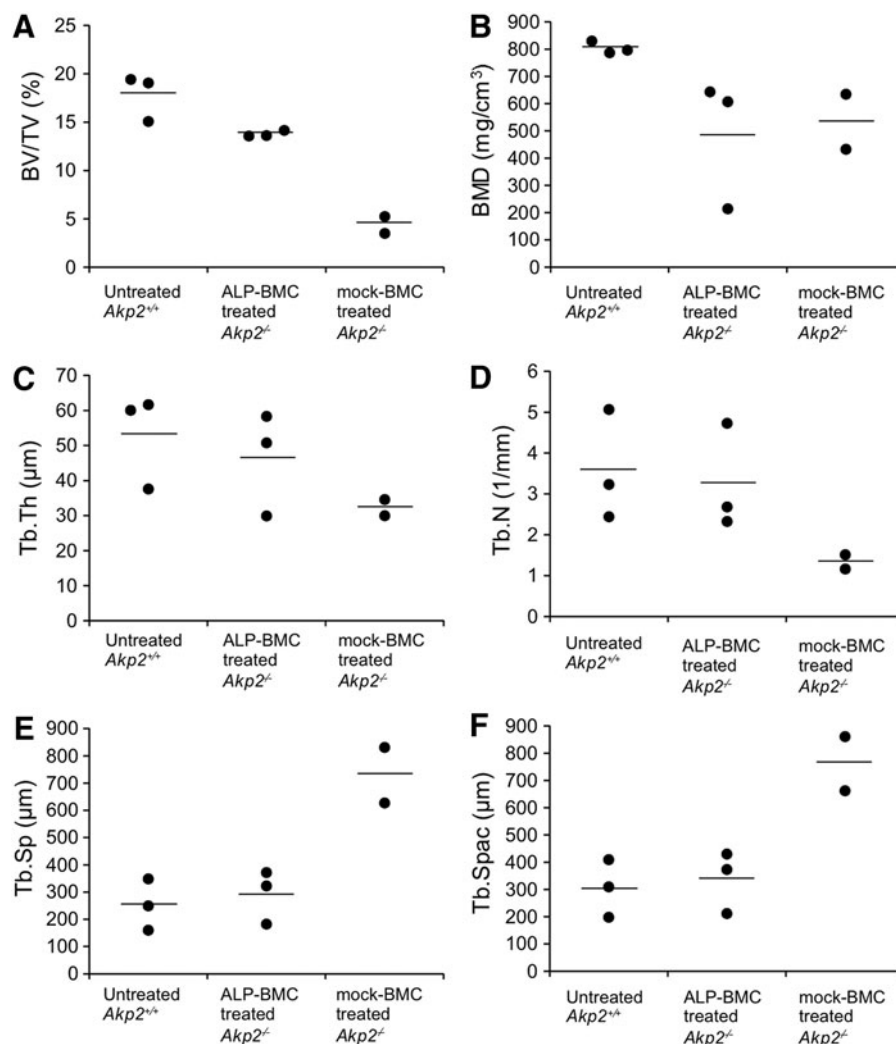


Figure 4. μ CT analysis of femoral bones. The trabecular structural parameters were calculated for 100-day-old untreated *Akp2*^{+/+} mice ($n=3$), ALP-BMC-treated *Akp2*^{-/-} mice ($n=3$), and mock-BMC-treated *Akp2*^{-/-} mice ($n=2$). BMD, bone mineral density; BV/TV, bone volume/total volume; Tb.N, trabecular number; Tb.Sp, trabecular separation; Tb.Spac, trabecular spacing; Tb.Th, trabecular thickness. Horizontal bars represent the mean values for each group.

supplementation of soluble TNALP and MSC expressing native form of TNALP for differentiation into physiologically active osteoblasts can provide synergistic effects in the treatment of HPP.

There is no established regimen of conditioning for BMT of neonatal mice, although lethal irradiation is the most widely used in mouse BMT experiments. We gave 4 Gy of TBI to neonatal *Akp2*^{-/-} mice in this study. In recipient mice, the engraftment of donor cells was maintained at approximately 30% throughout the experimental period (Fig. 1E). However, even low-dose irradiation may be toxic especially in the neonatal period and associated with risks of growth impairment (Fig. 1B) and/or neural cell damage.⁴² Recently, it was reported that various genetic diseases can be successfully treated by hematopoietic stem cell-based *ex vivo* gene therapy in which the immunosuppressive

drug busulfan or melphalan was used for the preconditioning.^{26,43–45} Thus, immunosuppressive drugs may also be applicable for the preconditioning before *ex vivo* gene therapy for HPP.

The transplanted ALP-BMC in the recipient *Akp2*^{-/-} mice showed stable engraftment (Fig. 1E) with normal multilineage reconstitution (Tables 1 and 2). This suggests that the overexpression of TNALP-D₁₀ did not affect reconstitution by the donor BMC. It has also been reported that overexpression of a therapeutic enzyme in lentivirally transduced BMC does not affect the hematopoietic system during *ex vivo* gene therapy in metachromatic leukodystrophy²⁶ or Pompe⁴⁶ and Fabry⁴⁷ disease. We therefore suggest that lentivirally transduced BMC can serve as an applicable reservoir for a safe, long-term supply of TNALP-D₁₀ with normal hematopoietic reconstitution. The

treated *Akp2*^{-/-} mice were normal in appearance, and no ectopic calcification was observed within internal organs. However, careful follow-up (e.g., monitoring of vascular calcification) is needed to assess the efficacy and safety of the stem cell-based ERT in future experiments.

Analysis of tissue ALP activity in ALP-BMC-treated *Akp2*^{-/-} mice revealed that, whereas similar amounts of lentiviral vector genome were present in spleen and bone, TNALP-D₁₀ localized exclusively in bone tissue (Fig. 2A and B). Additionally, histochemical detection of ALP activity in femurs revealed targeted accumulation of TNALP-D₁₀ on the surface of trabecular and cortical bone in the ALP-BMC-treated *Akp2*^{-/-} mice (Fig. 2C). These findings suggest that the TNALP-D₁₀ produced by transduced BMC accumulates on the surface of bone due to its high affinity for hydroxyapatite.^{3,17} On the other hand, virtually no localization of TNALP-D₁₀ was detected on growth plate chondrocytes in ALP-BMC-treated *Akp2*^{-/-} mice, whereas the growth plate chondrocytes of *Akp2*^{+/+} mice express abundant TNALP during bone development (Fig. 2C). X-ray and μ CT examination of the skeleton showed that bone formation was much improved in ALP-BMC-treated *Akp2*^{-/-} mice (Fig. 3A and B) and that the trabecular bone structure in ALP-BMC-treated *Akp2*^{-/-} mice was restored to levels similar to that in *Akp2*^{+/+} mice (Fig. 4). Nonetheless, immature bone formation, including a widened metaphysis, persisted in ALP-BMC-treated *Akp2*^{-/-} mice (Fig. 3A and B). These results indicate that the moderate accumulation of TNALP-D₁₀ on the bone surface was sufficient to enhance bone mineralization, but was not sufficient to mediate the formation of a normal metaphysis. Proliferative growth plate chondrocytes are reportedly abnormal in the articular and epiphyseal cartilage of *Akp2*^{-/-} mice treated with recombinant GPI-anchorless TNALP, though survival of these animals was prolonged over 6 months by the ERT.¹⁵ Thus, accumulation of TNALP on the surface of both bone and growth plate chondrocytes in the epiphyses is essential for normal bone formation.

Perinatal HPP is the most severe form of the disease, and efficacious treatment as early as possible is required for these patients. With development of prenatal diagnosis through the use of echography, computed tomography, and genetic diagnosis, perinatal HPP can be correctly diagnosed in the fetus before birth.^{48,49} To develop a fetal treatment for perinatal HPP, we previously examined the effect of transuterine intraperitoneal injection of an AAV vector harboring the *TNALP-D*₁₀

construct into fetal *Akp2*^{-/-} mice on day 15 of gestation.¹⁸ The fetal treatment provided preferential transduction of growth plate chondrocytes by AAV vector in the epiphysis of the treated *Akp2*^{-/-} mice. *In utero* transplantation of paternal hematopoietic stem cells was successfully applied to treat X-linked severe combined immunodeficiency.^{50,51} In addition, *in utero* transplantation of genetically modified BMC was also determined to be an applicable strategy for treating inherited disease model mice.^{52,53} If transplanted BMC migrate to nearby primordial cartilage in fetal bone in *Akp2*^{-/-} mice, it may be that TNALP-D₁₀ could be safely supplied at levels sufficient for chondrocyte differentiation early during fetal development. The possibility of *in utero* transplantation of BMC expressing TNALP-D₁₀ would be examined to determine whether genetically modified BMC can protect against the skeletal abnormalities and rescue perinatal *Akp2*^{-/-} mice.

In summary, we successfully applied stem cell-based ERT to treat the lethal phenotype of *Akp2*^{-/-} mice through a single systemic transplantation of lentivirally transduced BMC on day 2 after birth. Plasma ALP activity in the treated *Akp2*^{-/-} mice rapidly increased following transplantation and was maintained at a level sufficient to prolong survival with improved weight gain and bone mineralization. To achieve greater therapeutic efficacy leading to normal bone development, there will need to be improvements to the engraftment regimen and strategy for local delivery of TNALP onto the surface of bone matrix and growth plate chondrocytes. However, neonatal *ex vivo* gene therapy using BMC expressing TNALP-D₁₀ appears to be a potentially effective and beneficial means of continuously supplying TNALP-D₁₀ for the treatment of infantile HPP.

ACKNOWLEDGMENTS

We thank Dr. Seiko Yamamoto at the Nihon University Graduate School of Dentistry at Matsudo, and Dr. Tae Matsumoto and Dr. Hanako Sugano-Tajima at Nippon Medical School for valuable advice and support. This work was supported by JSPS KAKENHI Grant Number 25461564.

AUTHOR DISCLOSURE

J.L.M. is a consultant for Alexion Pharmaceuticals (Cheshire, CT) and AM Pharma (Bunnik, Netherlands). The other authors have no competing financial interests.

REFERENCES

1. Mornet E. Hypophosphatasia. *Orphanet J Rare Dis* 2007;2:40.
2. Whyte MP. Physiological role of alkaline phosphatase explored in hypophosphatasia. *Ann N Y Acad Sci* 2010;1192:190–200.
3. Millán JL. The role of phosphatases in the initiation of skeletal mineralization. *Calcif Tissue Int* 2013;93:299–306.
4. Whyte MP, Landt M, Ryan LM, et al. Alkaline phosphatase: Placental and tissue-nonspecific isoenzymes hydrolyze phosphoethanolamine, inorganic pyrophosphate, and pyridoxal 5'-phosphate. Substrate accumulation in carriers of hypophosphatasia corrects during pregnancy. *J Clin Invest* 1995;95:1440–1445.
5. Fedde KN, Lane CC, Whyte MP. Alkaline phosphatase is an ectoenzyme that acts on micromolar concentrations of natural substrates at physiologic pH in human osteosarcoma (SAOS-2) cells. *Arch Biochem Biophys* 1988;264:400–409.
6. Kozłowski K, Sutcliffe J, Barylak A, et al. Hypophosphatasia. Review of 24 cases. *Pediatr Radiol* 1976;5:103–117.
7. Whyte MP, Zhang F, Wenkert D, et al. Hypophosphatasia: Validation and expansion of the clinical nosology for children from 25 years experience with 173 pediatric patients. *Bone* 2015; 75:229–239.
8. Demirbilek H, Alanay Y, Alikafıoğlu A, et al. Hypophosphatasia presenting with pyridoxine-responsive seizures, hypercalcemia, and pseudotumor cerebri: Case report. *J Clin Res Pediatr Endocrinol* 2012;4:34–38.
9. Cahill RA, Wenkert D, Perlman SA, et al. Infantile hypophosphatasia: Transplantation therapy trial using bone fragments and cultured osteoblasts. *J Clin Endocrinol Metab* 2007;92: 2923–2930.
10. Tadokoro M, Kanai R, Taketani T, et al. New bone formation by allogeneic mesenchymal stem cell transplantation in a patient with perinatal hypophosphatasia. *J Pediatr* 2009;154:924–930.
11. Taketani T, Oyama C, Mihara A, et al. Ex vivo expanded allogeneic mesenchymal stem cells with bone marrow transplantation improved osteogenesis in infants with severe hypophosphatasia. *Cell Transplant* 2015;24:1931–1943.
12. Whyte MP, Kurtzberg J, McAlister WH, et al. Marrow cell transplantation for infantile hypophosphatasia. *J Bone Miner Res* 2003;18:624–636.
13. Millán JL, Narisawa S, Lemire I, et al. Enzyme replacement therapy for murine hypophosphatasia. *J Bone Miner Res* 2008;23:777–787.
14. Whyte MP, Greenberg CR, Salman NJ, et al. Enzyme-replacement therapy in life-threatening hypophosphatasia. *N Engl J Med* 2012;366:904–913.
15. Oikawa H, Tomatsu S, Haupt B, et al. Enzyme replacement therapy on hypophosphatasia mouse model. *J Inher Metab Dis* 2014;37:309–317.
16. Gasque KC, Foster BL, Kuss P, et al. Improvement of the skeletal and dental hypophosphatasia phenotype in *Alpl*^{-/-} mice by administration of soluble (non-targeted) chimeric alkaline phosphatase. *Bone* 2015;72:137–147.
17. Matsumoto T, Miyake K, Yamamoto S, et al. Rescue of severe infantile hypophosphatasia mice by AAV-mediated sustained expression of soluble alkaline phosphatase. *Hum Gene Ther* 2011;22:1355–1364.
18. Sugano H, Matsumoto T, Miyake K, et al. Successful gene therapy *in utero* for lethal murine hypophosphatasia. *Hum Gene Ther* 2012;23:399–406.
19. Yamamoto S, Orimo H, Matsumoto T, et al. Prolonged survival and phenotypic correction of *Akp2*^(-/-) hypophosphatasia mice by lentiviral gene therapy. *J Bone Miner Res* 2011;26:135–142.
20. Porada CD, Park PJ, Tellez J, et al. Male germ-line cells are at risk following direct-injection retroviral-mediated gene transfer *in utero*. *Mol Ther* 2005;12:754–762.
21. Schuettrumpf J, Liu JH, Couto LB, et al. Inadvertent germline transmission of AAV2 vector: Findings in a rabbit model correlate with those in a human clinical trial. *Mol Ther* 2006;13:1064–1073.
22. Nathwani AC, Tuddenham EG, Rangarajan S, et al. Adenovirus-associated virus vector-mediated gene transfer in hemophilia B. *N Engl J Med* 2011;365:2357–2365.
23. Wu T, Töpfer K, Lin SW, et al. Self-complementary AAVs induce more potent transgene product-specific immune responses compared to a single-stranded genome. *Mol Ther* 2012;20:572–579.
24. Ginn SL, Alexander IE, Edelstein ML, et al. Gene therapy clinical trials worldwide to 2012—an update. *J Gene Med* 2013;15:65–77.
25. Mukherjee S, Thrasher AJ. Gene therapy for PIDs: Progress, pitfalls and prospects. *Gene* 2013;525: 174–181.
26. Biffi A, Montini E, Lorioli L, et al. Lentiviral hematopoietic stem cell gene therapy benefits metachromatic leukodystrophy. *Science* 2013;341: 1233158.
27. Hofling AA, Devine S, Vogler C, et al. Human CD34+ hematopoietic progenitor cell-directed lentiviral-mediated gene therapy in a xenotransplantation model of lysosomal storage disease. *Mol Ther* 2004;9:856–865.
28. Yoshimitsu M, Higuchi K, Ramsurir S, et al. Efficient correction of Fabry mice and patient cells mediated by lentiviral transduction of hematopoietic stem/progenitor cells. *Gene Ther* 2007; 14:256–265.
29. Scaramuzza S, Biasco L, Ripamonti A, et al. Pre-clinical safety and efficacy of human CD34(+) cells transduced with lentiviral vector for the treatment of Wiskott-Aldrich syndrome. *Mol Ther* 2013;21: 175–184.
30. Persons DA, Baum C. Solving the problem of gamma-retroviral vectors containing long terminal repeats. *Mol Ther* 2011;19:229–231.
31. Narisawa S, Fröhlander N, Millán JL. Inactivation of two mouse alkaline phosphatase genes and establishment of a model of infantile hypophosphatasia. *Dev Dyn* 1997;208:432–446.
32. Narisawa S, Wennberg C, Millán JL. Abnormal vitamin B6 metabolism in alkaline phosphatase knock-out mice causes multiple abnormalities, but not the impaired bone mineralization. *J Pathol* 2001;193:125–133.
33. Miyake N, Brun AC, Magnusson M, et al. HOXB4-induced self-renewal of hematopoietic stem cells is significantly enhanced by p21 deficiency. *Stem Cells* 2006;24:653–661.
34. Hanawa H, Yamamoto M, Zhao H, et al. Optimized lentiviral vector design improves titer and transgene expression of vectors containing the chicken beta-globin locus HS4 insulator element. *Mol Ther* 2009;17:667–674.
35. Charrier S, Dupré L, Scaramuzza S, et al. Lentiviral vectors targeting WASp expression to hematopoietic cells, efficiently transduce and correct cells from WAS patients. *Gene Ther* 2007;14:415–428.
36. Kawamoto T. Use of a new adhesive film for the preparation of multi-purpose fresh-frozen sections from hard tissues, whole-animals, insects and plants. *Arch Histol Cytol* 2003;66:123–143.
37. Kinoshita H, Nakahara K, Matsunaga S, et al. Association between the peri-implant bone structure and stress distribution around the mandibular canal: A three-dimensional finite element analysis. *Dent Mater J* 2013;32:637–642.
38. Nakamura-Utsunomiya A, Okada S, Hara K, et al. Clinical characteristics of perinatal lethal hypophosphatasia: A report of 6 cases. *Clin Pediatr Endocrinol* 2010;19:7–13.
39. Shohat M, Rimoin DL, Gruber HE, et al. Perinatal lethal hypophosphatasia; clinical, radiologic and morphologic findings. *Pediatr Radiol* 1991;21:421–427.
40. Ciancaglini P, Yadav MC, Simão AM, et al. Kinetic analysis of substrate utilization by native and TNAP-, NPP1-, or PHOSPHO1-deficient matrix vesicles. *J Bone Miner Res* 2010;25:716–723.
41. Katsube Y, Kotobuki N, Tadokoro M, et al. Restoration of cellular function of mesenchymal stem cells from a hypophosphatasia patient. *Gene Ther* 2010;17:494–502.

42. Igarashi T, Miyake K, Hayakawa J, et al. Apoptotic cell death and regeneration in the newborn retina after irradiation prior to bone marrow transplantation. *Curr Eye Res* 2007;32:543–553.
43. Candotti F, Shaw KL, Muul L, et al. Gene therapy for adenosine deaminase-deficient severe combined immune deficiency: Clinical comparison of retroviral vectors and treatment plans. *Blood* 2012;120:3635–3646.
44. Cartier N, Hacein-Bey-Abina S, Bartholomae CC, et al. Hematopoietic stem cell gene therapy with a lentiviral vector in X-linked adrenoleukodystrophy. *Science* 2009;326:818–823.
45. Hacein-Bey-Abina S, Hauer J, Lim A, et al. Efficacy of gene therapy for X-linked severe combined immunodeficiency. *N Engl J Med* 2010;363:355–364.
46. van Til NP, Stok M, Aerts Kaya FS, et al. Lentiviral gene therapy of murine hematopoietic stem cells ameliorates the Pompe disease phenotype. *Blood* 2010;115:5329–5337.
47. Pacienza N, Yoshimitsu M, Mizue N, et al. Lentivector transduction improves outcomes over transplantation of human HSCs alone in NOD/SCID/Fabry mice. *Mol Ther* 2012;20:1454–1461.
48. Mornet E, Hofmann C, Bloch-Zupan A, et al. Clinical utility gene card for: Hypophosphatasia—update 2013. *Eur J Hum Genet* 2014;22:e1–e6.
49. Watanabe A, Yamamasu S, Shinagawa T, et al. Prenatal genetic diagnosis of severe perinatal (lethal) hypophosphatasia. *J Nippon Med Sch* 2007;74:65–69.
50. Flake AW, Roncarolo MG, Puck JM, et al. Treatment of X-linked severe combined immunodeficiency by *in utero* transplantation of paternal bone marrow. *N Engl J Med* 1996;335:1806–1810.
51. Wengler GS, Lanfranchi A, Frusca T, et al. *In-utero* transplantation of parental CD34 haematopoietic progenitor cells in a patient with X-linked severe combined immunodeficiency (SCIDX1). *Lancet* 1996;348:1484–1487.
52. Rio P, Martinez-Palacio J, Ramirez A, et al. Efficient engraftment of *in utero* transplanted mice with retrovirally transduced hematopoietic stem cells. *Gene Ther* 2005;12:358–363.
53. Meza NW, Alonso-Ferrero ME, Navarro S, et al. Rescue of pyruvate kinase deficiency in mice by gene therapy using the human isoenzyme. *Mol Ther* 2009;17:2000–2009.

Received for publication May 27, 2015;
accepted after revision October 1, 2015.

Published online: October 14, 2015.